International Journal of Applied Science and Engineering
2006. 4, 1: 53-69

Seismic Response of Simply Supported Base-Isolated Bridge with Different Isolators

Vasant A. Matsagar and R. S. Jangid*

Department of Civil Engineering,
Indian Institute of Technology Bombay, Powai, Mumbai - 400 076, India

Abstract: The seismic response of simply supported base-isolated bridge with different isolators is presented. The isolated bridge deck is idealized using simplified model of a simply supported rigid deck with three degrees-of-freedom, two lateral translational, mutually orthogonal and one rotational. The rotational degree-of-freedom of the bridge deck may arise because of the dissimilarity in properties of different seismic isolation devices such as elastomeric and sliding systems supporting the bridge deck. The sources of dissimilarity in the isolators considered here are the isolation stiffness and the yield force. The flexibility of abutments and bridge deck is ignored and two horizontal components of earthquake ground motion are applied, considering bi-directional interaction of the seismic response. The governing equations of motion for the uncoupled and torsionally coupled bridge are derived and solved using Newmark's method of integration to obtain the seismic response. The parametric studies are conducted for different system configurations, isolation systems and frequency ratios during torsionally coupled and uncoupled conditions. The seismic response of base-isolated bridge is seen to be considerably altered due to the dissimilarity in the isolator properties. The eccentricity arose due to the isolation stiffness affects more than that due to the isolator yield forces. The effectiveness of isolation reduces at higher eccentricities and the torsionally coupled response diminishes with the increase of uncoupled torsional to lateral frequency ratio.

Keywords: asymmetry; base isolation; bridge; earthquake; eccentricity; torsional coupling.

1. Introduction

Bridges serve in the surface transport and carries water supply, electric lines across a stream. Apart from these day-to-day amenity services, during natural calamities such as earthquakes, it facilitates in providing the emergency services like supply of food, medicine etc.; hence, the bridges are lifeline structures. The relief and rehabilitation work is made possible only if bridges are saved from failures during earthquake events. However, due to lack of structural redundancy bridges receive severe damage and generally lead to catastrophic failures during earthquakes. For the bridges with relatively short piers, the natural frequency of vibration lies in the range of pre-dominant frequencies of the earthquake ground motions, particularly when founded on rock or hard soil. Merely increasing the strength of members will not be effective and uneconomical too, unless the transmission of the earthquake forces and energy into the structure is reduced. Therefore, base isolation devices (seismic isolators) may replace the conventional bridge

* Corresponding author; e-mail: rsjangid@civil.iitb.ac.in *Accepted for Publication: March 07, 2006*

bearings, lengthening the natural vibration time period (i.e. detuning) and supplying means of hysteretic energy dissipation. Such isolation devices decouple the bridge deck (which is responsible for development of base shear in the supporting abutments and piers) from bridge substructure during earthquakes, consequently reducing the forces transmitted to abutments and piers. Thus, the bridge is protected against damage from the earthquake by limiting the earthquake attack rather than resisting it.

The foremost design variable for seismic isolation systems is the isolator displacement along with other variables like, bridge deck acceleration, abutment/pier shear force etc. These response quantities provide vital information such as: (i) the isolation gap required between the junction of two bridge decks to facilitate unrestricted movement, avoiding problems of pounding and dislodgement in case of simply supported bridge; (ii) the requirement of isolator plan dimension; (iii) the strains developed in isolator in shear and its structural stability; and (iv) the extent of forces transmitted to the bridge substructure. The estimation of displacements through two-dimensional (2D) planar idealization will be accurate only if bridges are supported on seismic isolators with exactly identical properties, making it symmetrical. The real bridges however are asymmetrical on account of their dissimilarity in the isolation stiffness distributions and/ or the attainment of yield force levels, which are most likely manufacturing faults. The bridges excited by earthquakes undergo lateral as well as torsional motions, if the center of mass (CM) and center of rigidity (CR) mismatch at the bridge deck level. The bridge may experience highly increased response when the line joining CM and CR is perpendicular to the direction of earthquake excitation. Hence, for such bridges a three-dimensional (3D) analysis is essential to obtain the accurate design displacements and forces. Several studies [1-6] had been reported in the past on the effectiveness base isolation for bridges for different types of isolation systems. Currently, the seismic isolation had been successfully implemented in the actual practice. Reference [7] provides detailed review on analytical and experimental studies on effectiveness of seismic isolation and its implementation in actual bridges. It is to be noted that most of the past studies on the bridge were conducted by ignoring the effects of torsional couplings due to isolation systems. However, such effects can play crucial role in the seismic response of isolated structural system [8-11]. In this context, it is important to investigate the performance of different isolation systems used for bridges and study the effects of eccentricities in the restoring forces provided by the isolation systems.

The present study aims at identifying the important system parameters affecting the lateral-torsional response of a simply supported bridge, while putting forth simplified analysis approach. The specific objectives of the study are to: (i) formulate the asymmetries in the base-isolated bridge due to the isolation stiffness and the yield forces; and (ii) to study various parameters affecting response of the torsionally coupled base-isolated bridges.

2. Mathematical model

A non-linear response-history analysis in time domain is employed in this study on a base-isolated bridge, idealized as a rigid deck, ignoring flexibility in bridge deck and the supporting abutments/ piers as shown in Figure 1. These assumptions do not affect the response quantities to a greater extent, as demonstrated previously [12]. This simplified mathematical model of base-isolated single-span bridge is considered excited under two horizontal components of earthquake ground motion, applied simultaneously and the interaction of responses obtained along the two orthogonal directions is duly considered [8]. However, the velocity dependence of response in sliding systems is omitted, be-

cause it has meager effect as compared to the bi-directional interaction [9]. Similarly, it is to be noted that for a multi-span simply supported bridge (as shown in the inset of Figure 1), any single span can also be represented with the present model. Such simplified mathematical model facilitates clear understanding of the behavior of system under investigation and adopted in the past studies made on asymmetries in the base-isolated structures [10, 11].

The bridge deck of plan dimensions $b = 21.4\,\text{m} \times d = 30\,\text{m}$ is considered mounted on various types of seismic isolation systems. The thickness of bridge deck is assumed equal to $0.5\,\text{m}$ made of concrete of density $2.4 \times 10^4\ \text{N/m}^3$; thus, making total weight of bridge deck equal to $7.704 \times 10^3\ \text{kN}$. The CR provided by the isolator restoring forces does not coincide with the CM of the bridge deck due to either of: (i) the variation in the stiffness, k_b of the isolation systems; (iii) variation in the yield forces, f^y or friction coefficients, μ in the elastomeric or sliding isolation systems, respectively. These eccentricities are labeled as 'isolation eccentricities'. The uni-directional eccentricities in longitudinal *x*-direction are considered, as recommended important [13]; while soil-structure and structure-water interactions ignored.

The CR provided by the isolation system is a resultant of the restoring forces developed in the individual isolators placed below the bridge deck. With the differences in the isolation stiffness and/ or the yield forces (or friction coefficients) of the individual isolators, the resultant CR of all the isolators does not coincide with the CM of the bridge deck. Hence, due to such isolation eccentricities, the seismic response of the bridge is affected, showing the torsional coupling. Let k_{xbj} and k_{ybj} represent the lateral isolation stiffness and f_{xj} and f_{yj} represent the isolation forces in the j^{th} isolator developed in *x*- and *y*-directions, respectively. Then

$$K_{xb} = \sum_j k_{xbj}\ ; \text{ and } \ K_{yb} = \sum_j k_{ybj} \qquad (1)$$

are the total lateral stiffness of the isolation system in the *x*- and *y*-directions, respectively; whereas, the total restoring force component in *x*- and *y*-directions, respectively is represented as

$$F_x = \sum_j f_{xj}\ ; \text{ and } \ F_y = \sum_j f_{yj} \qquad (2)$$

Hence, the torsional force developed due to the isolation system, defined about the vertical axis passing through the CM of the bridge deck, is given by $F_\theta = \sum_j \left(f_{xj}\, y_j + f_{yj}\, x_j \right)$; where x_j and y_j denote the *x*- and *y*- coordinates of the j^{th} isolator with respect to the CM of the bridge deck, respectively. The torsional stiffness of the isolation system defined about the vertical axis passing through the CM of the bridge deck is given by

$$K_\theta = \sum_j \left(k_{xbj}\, y_j^2 + k_{ybj}\, x_j^2 \right) \qquad (3)$$

The torsional stiffness of each individual isolation system is negligible, hence ignored. The uncoupled frequency parameters of the system are defined as follows

$$\omega_x = \sqrt{\frac{K_{xb}}{m}}\ ; \ \ \omega_y = \sqrt{\frac{K_{yb}}{m}}\ ; \text{ and } \ \omega_\theta = \sqrt{\frac{K_\theta}{m r^2}} \qquad (4)$$

where *m* and *r* are the mass and radius of gyration of the bridge deck about the vertical axis passing through the CM of the bridge deck, respectively. The frequencies ω_x, ω_y and ω_θ are the natural frequencies of the isolation system if it would have been torsionally uncoupled, i.e. a system with $e_x = 0$, having *m*, K_{xb}, K_{yb} and K_θ same as in the torsionally coupled system. Here, the total eccentricity between the CM of bridge deck and the CR of the isolators is $e_x = e_{xb} + e_{xf}$ considered in the longitudinal *x*-direction. The eccentricity arising due to dissimilarity in

isolation stiffness is expressed as

$$e_{\mathrm{xb}} = \frac{1}{K_{\mathrm{yb}}} \sum_{j} k_{\mathrm{ybj}}\, x_{\mathrm{j}} \tag{5}$$

Whereas, the isolation eccentricity arising due to the differences in yield forces is expressed as

$$e_{\mathrm{xf}} = \frac{1}{F^{\mathrm{y}}} \sum_{j} f_{\mathrm{j}}^{\mathrm{y}}\, x_{\mathrm{j}} \tag{6}$$

where F^{y} is the total yield force of all bearings; and $f_{\mathrm{j}}^{\mathrm{y}}$ is the yield force level of j^{th} bearing. The restoring forces developed in the different isolation systems can be expressed as follows.

2.1. Laminated rubber bearing

The popularly used laminated rubber bearings (LRB) comprise of steel and rubber plates built in the alternate layers, represented by a linear spring and viscous damper acting in parallel [14]. The LRB is characterized with high damping capacity, horizontal flexibility and high vertical stiffness. Sectional view of a typical LRB, its schematic diagram for bi-directional excitation and the ideal force-deformation curve is shown in Figure 2(a). The restoring forces developed in the LRB are

$$\begin{Bmatrix} f_{\mathrm{xj}} \\ f_{\mathrm{yj}} \end{Bmatrix} = \begin{bmatrix} c_{\mathrm{xbj}} & 0 \\ 0 & c_{\mathrm{ybj}} \end{bmatrix} \begin{Bmatrix} \dot{u}_{\mathrm{xj}} \\ \dot{u}_{\mathrm{yj}} \end{Bmatrix} + \begin{bmatrix} k_{\mathrm{xbj}} & 0 \\ 0 & k_{\mathrm{ybj}} \end{bmatrix} \begin{Bmatrix} u_{\mathrm{xj}} \\ u_{\mathrm{yj}} \end{Bmatrix} \tag{7}$$

where c_{xbj} and c_{ybj} are the viscous damping coefficients; k_{xbj} and k_{ybj} are the stiffness coefficients of LRB, respectively in *x*- and *y*-directions for the j^{th} isolator. $\dot{u}_{\mathrm{xj}}$ and $\dot{u}_{\mathrm{yj}}$ represent relative velocity; also, u_{xj} and u_{yj} represent the relative displacement in *x*- and *y*- direction of the bridge, respectively. The isolation properties in the *x*- and *y*-direction are similar for an orthotropic isolator; hence, $c_{\mathrm{xbj}} = c_{\mathrm{ybj}}$ and $k_{\mathrm{xbj}} = k_{\mathrm{ybj}}$. Therefore, note that the isolation time period, T_{b} and the isolation damping, ξ_{b} in all the directions remain the same.

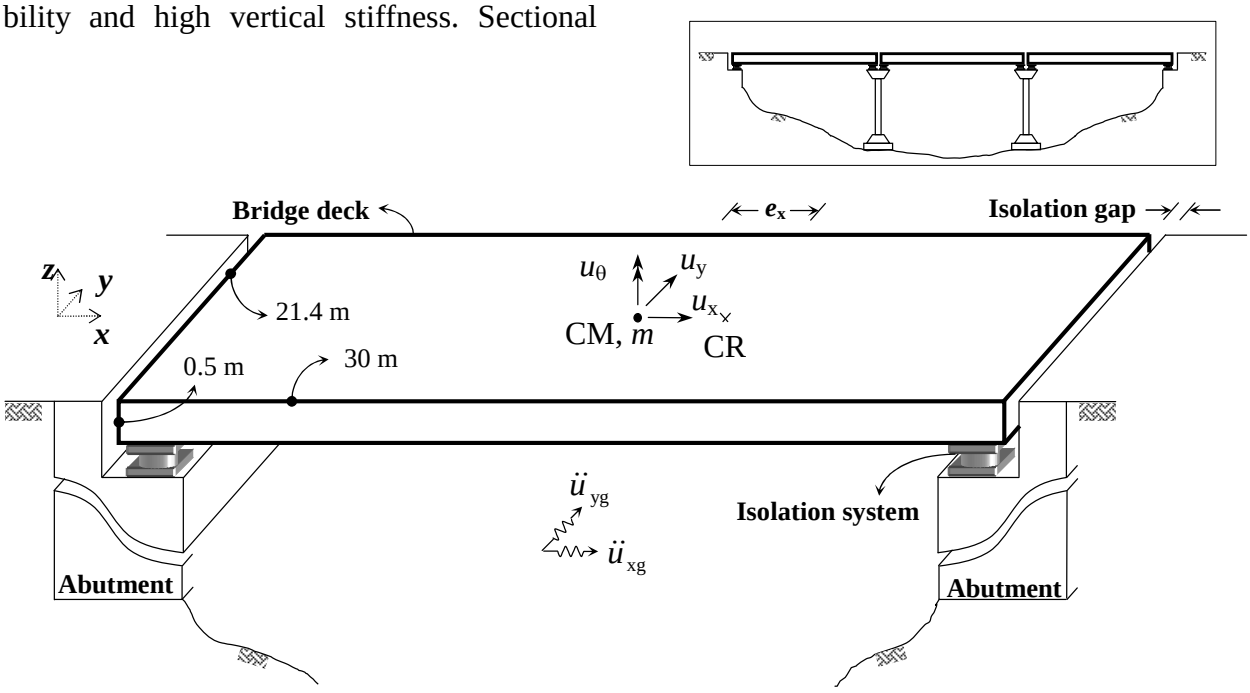

Figure 1. Mathematical model of the base-isolated bridge marked with eccentricities.

The stiffness and damping of the LRB is selected to provide the specified values of the two parameters namely, the isolation time period (T_b) and damping ratio (ξ_b) defined as

$$T_b = 2\pi\sqrt{\frac{m}{K_{xb}}}\ ;\ \text{and}\ \ \xi_b = \frac{\sum_j c_{xbj}}{2\,m\,\omega_x} \qquad (8)$$

2.2. where $\omega_x = 2\pi/T_b$ is the isolation frequency in longitudinal direction of the bridge.**Lead-rubber bearing**

Except using a central lead-core to provide additional means of energy dissipation and initial rigidity against minor earthquakes and winds [15, 16], lead-rubber bearings are similar to the LRB. These isolators are widely developed and used in New Zealand; hence, referred as N-Z systems. The N-Z isolators provide an additional hysteretic damping through the yielding of lead-core. The sectional view, schematic diagram for bi-directional excitation and the ideal force-deformation curve of the N-Z isolator is shown in Figure 2(b). For the present study, Park-Wen's model [17] for bi-directional excitation is used to characterize the hysteretic behavior of the N-Z isolators. This model had been widely used for N-Z system in the past [6, 18, 19]. The restoring forces developed in the N-Z isolator are

$$\begin{Bmatrix} f_{xj} \\ f_{yj} \end{Bmatrix} = \begin{bmatrix} c_{xbj} & 0 \\ 0 & c_{ybj} \end{bmatrix} \begin{Bmatrix} \dot{u}_{xj} \\ \dot{u}_{yj} \end{Bmatrix} + \alpha \begin{bmatrix} k_{xj} & 0 \\ 0 & k_{yj} \end{bmatrix} \begin{Bmatrix} u_{xj} \\ u_{yj} \end{Bmatrix} + (1-\alpha) \begin{bmatrix} f_{xj}^{y} & 0 \\ 0 & f_{yj}^{y} \end{bmatrix} \begin{Bmatrix} Z_{xj} \\ Z_{yj} \end{Bmatrix} \qquad (9)$$

where f_{xj}^{y} and f_{yj}^{y} are the yield forces; k_{xj} and k_{yj} are the pre-yield stiffness coefficients of the j^{th} isolator in *x*- and *y*-directions, respectively; α is an index which represent the ratio of post to pre-yielding stiffness; whereas, Z_{xj} and Z_{yj} are the non-dimensional hysteretic displacement components satisfying the following non-linear first order differential equation

$$q_j \begin{Bmatrix} \dot{Z}_{xj} \\ \dot{Z}_{yj} \end{Bmatrix} = \begin{bmatrix} A-\beta\,\mathrm{sgn}(\dot{u}_x)\left|Z_{xj}\right|Z_{xj} - \tau Z_{xj}^2 & -\beta\,\mathrm{sgn}(\dot{u}_y)\left|Z_{yj}\right|Z_{xj} - \tau Z_{xj}Z_{yj} \\ -\beta\,\mathrm{sgn}(\dot{u}_x)\left|Z_{xj}\right|Z_{yj} - \tau Z_{xj}Z_{yj} & A-\beta\,\mathrm{sgn}(\dot{u}_y)\left|Z_{yj}\right|Z_{yj} - \tau Z_{yj}^2 \end{bmatrix} \begin{Bmatrix} \dot{u}_x \\ \dot{u}_y \end{Bmatrix} \qquad (10)$$

where q_j is the isolator yield displacement. The dimensionless parameters *A*, β and τ are selected such that the predicted response from mathematical model of the isolator closely matches with the experimental results.

The N-Z system is characterized by the isolation time period (T_b), damping ratio (ξ_b) and the normalized yield forces, i.e. $f_{xj}^{y}/W_d = f_{yj}^{y}/W_d = f_j^{y}/W_d$. Here, $W_d = m\,g$ is the total weight of the bridge deck; and *g* is the gravitational acceleration. The isolation parameters T_b and ξ_b are computed from Eq. (8) using the post-yield isolation stiffness, k_{xbj}. The other parameters of the N-Z system are held constant with q_j=2.5 cm, *A*=1 and $\beta = \tau = 0.5$.

2.3. Friction pendulum system

The concept of sliding systems used along with notion of a pendulum type response, by means of an articulated slider on spherical concave chrome surface, marks the friction pendulum system (FPS) [20]. The system is activated when the earthquake forces overcome the static value of friction, μ. The FPS develops a lateral force equal to the combination of the mobilized frictional force and the restoring force that develops because of rising of the bridge deck along the spherical surface. The sectional view, schematic diagram for bi-directional excitation and the ideal force-deformation curve of FPS is shown in Figure 2(c). The restoring forces provided by the FPS are

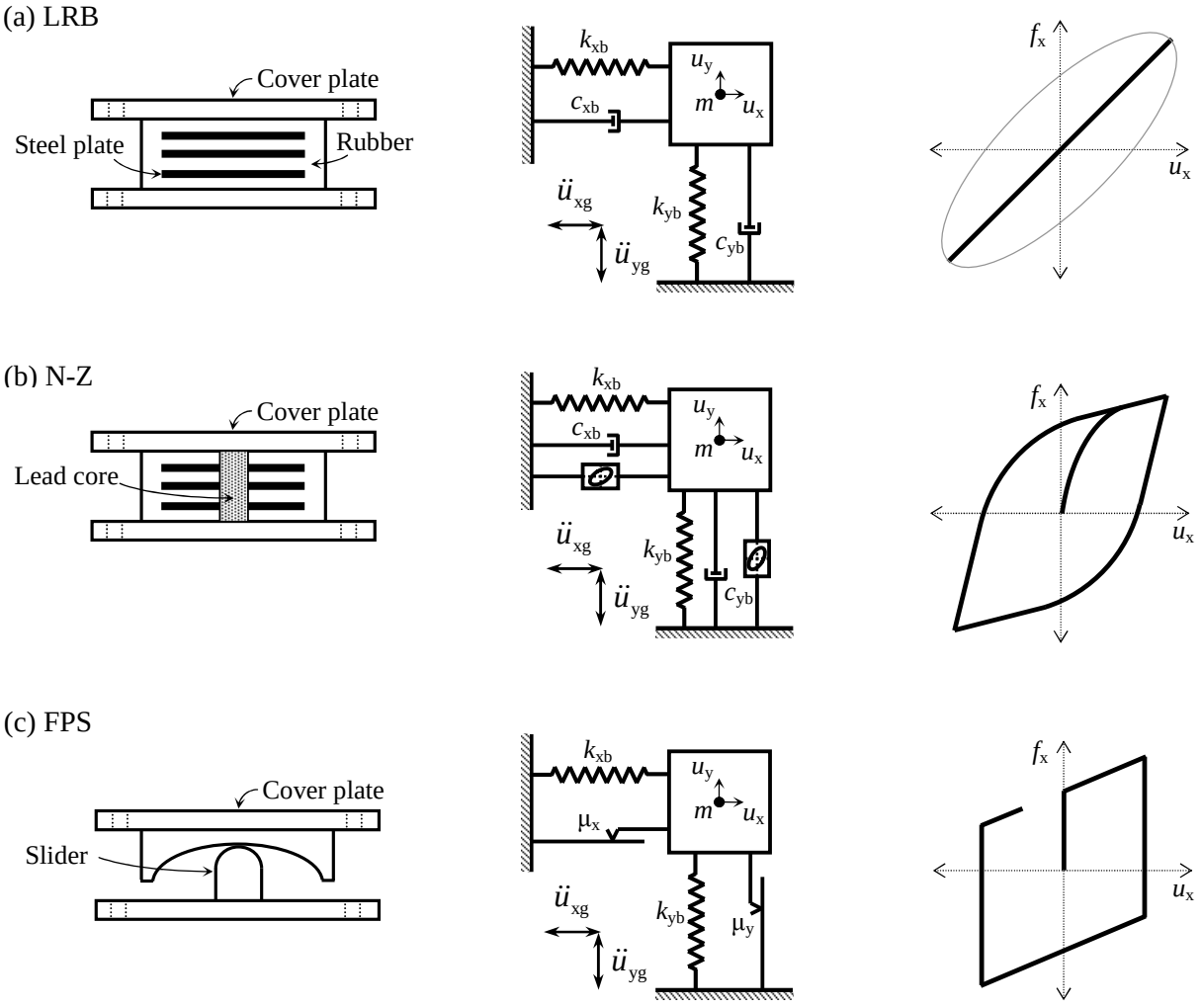

Figure 2. Sectional views, schematic diagrams and ideal force-deformation curves of different isolators.

$$\begin{Bmatrix} f_{xj} \\ f_{yj} \end{Bmatrix} = \begin{Bmatrix} f_{xj}^{y} \\ f_{yj}^{y} \end{Bmatrix} + \begin{bmatrix} k_{xbj} & 0 \\ 0 & k_{ybj} \end{bmatrix} \begin{Bmatrix} u_{xj} \\ u_{yj} \end{Bmatrix} \tag{11}$$

where k_{xbj} and k_{ybj} are the equivalent isolator stiffness provided by virtue of inward gravity action at the concave surface; whereas, $f_{xj}^{y} = \mu_x W_d$ and $f_{yj}^{y} = \mu_y W_d$ are the frictional forces in *x*- and *y*-directions, respectively.

The system is characterized by the isolation time period (T_b) that depends upon radius of curvature of the concave surface; and the friction coefficient ($\mu = \mu_x = \mu_y$). The isolation stiffness, k_{xbj} is adjusted such that the specified value of the isolation time period evaluated by the Eq. (8) is achieved.

3. Governing equations of motion and solution

The dynamic behavior of the bridge considered in the present study is described using three degrees-of-freedom such as, translation in the *x*- and *y*-directions and the rotation, θ about the CM. The governing equations of motion for the base-isolated bridge deck under bi-directional ground excitation are

$$\begin{bmatrix} m & 0 & 0 \\ 0 & m & 0 \\ 0 & 0 & m r^2 \end{bmatrix} \begin{Bmatrix} \ddot{u}_x \\ \ddot{u}_y \\ \ddot{u}_\theta \end{Bmatrix} + [C] \begin{Bmatrix} \dot{u}_x \\ \dot{u}_y \\ \dot{u}_\theta \end{Bmatrix} + \begin{Bmatrix} F_x \\ F_y \\ F_\theta \end{Bmatrix} = - \begin{bmatrix} m & 0 & 0 \\ 0 & m & 0 \\ 0 & 0 & m r^2 \end{bmatrix} \begin{Bmatrix} \ddot{u}_{xg} \\ \ddot{u}_{yg} \\ 0 \end{Bmatrix} \tag{12}$$

where $u_\theta = r\theta$ is the torsional displacement expressed in terms of the rotation; $[C]$ is the damping matrix; $\ddot{u}_{xg}$ and $\ddot{u}_{yg}$ are the ground acceleration in *x*- and *y*-direction, respectively.

The eccentricity in transverse *y*-direction, $e_y = 0$ implies a one-way eccentric system. The other system parameters considered for the bridge with the isolation eccentricity, hence can be summarized as follows.

The frequency ratio, Ω between the torsional and lateral frequencies expressed as

$$\Omega = \frac{\omega_\theta}{\omega_x} = \frac{\omega_\theta}{\omega_y} \tag{13}$$

Whereas, the other system parameter is of eccentricity expressed in terms of eccentricity ratio, normalized with the plan dimension, *d* as e_x / d. The displacement of the deck corner is given by

$$u_c(t) = u_x(t) \pm \frac{b}{2r} u_\theta(t) \tag{14}$$

The force-deformation relationships for the seismic isolation systems are non-linear (hysteretic) therefore, an iterative procedure is required at each time step to solve the equation of motion (Eq. 12). Therefore, the governing equation of motion is solved numerically using Newmark's method of step-by-step integration, adopting linear variation of acceleration over a small time interval of δt. The time interval for solving the equations of motion is taken as 0.02/20 sec (i.e. δt = 0.001 sec).

4. Numerical study

The objective here is to study the different parameters affecting the seismic response of a base-isolated bridge torsionally coupled on account of the isolation properties. Results of the response-history analyses in time domain gives the maximum displacements across the isolation interface at the CM of bridge deck (assuming rigid); acceleration induced in the bridge deck; shear force developed in the abutments/ piers; and displacement of corner of the bridge deck. The system considered in the present study can be completely characterized by the parameters such as ω_x, Ω, e_x / d and the isolator parameters; note that eccentricities are considered only along longitudinal *x*-direction. The three earthquake ground motions selected from firm soil/ hard rock sites for the present study are summarized in Table 1, showing also the direction in which those are applied to the bridge. The displacement and acceleration response spectra of the above ground motions for 2% of the critical damping are shown in Figure 3. The peak values of the spectra lies in the vicinity of 0.5 sec indicating that these ground motions are recorded at firm soil or rock sites.

The peak values of the abutment base shear (normalized with deck weight), acceleration induced, and displacement of the bridge deck are shown in Table 2 under the selected three earthquake ground motions. It includes the seismic response obtained for the non-isolated and base-isolated bridge, with and without asymmetries. The isolation systems utilized are LRB ($T_b = 2\,\text{sec}$ and $\xi_b = 0.1$); N-Z ($T_b = 2.5\,\text{sec}$, $\xi_b = 0.05$, $q_j = 2.5\,\text{cm}$ and $f_j^y / W_d = 0.05$); and FPS ($T_b = 2.5\,\text{sec}$ and $\mu = 0.05$). The torsional coupling parameters selected are: isolation eccentricities, $e_{xb} / d = 0.2$, $e_{xf} / d = 0.2$ and frequency ratio, $\Omega = 0.8$. From these tabulated results, it is observed that the torsionally coupled seismic responses in the base-isolated bridge dif-

fer substantially from that when no torsional coupling exists. When the torsional coupling is considered, the peak values of base shear developed in the abutment, acceleration induced, and displacement of the bridge deck have decreased than in the absence of torsional coupling. Thus, the effectiveness of isolation is over-predicted when eccentricities are not considered in the analysis. The comparison of seismic responses obtained for non-isolated and base-isolated bridge shows the effectiveness of isolation.

Table 1. Properties of the earthquake ground motions selected.

Earthquake	Event	Recording station	Component	PGA* (*g*)
Loma Prieta, 1989	October 18th, 1989	Los Gatos Presentation Center	N00E (Longitudinal)	0.559
			N90E (Transverse)	0.596
Northridge, 1994	January 17th, 1994	Sylmar	N90S (Longitudinal)	0.593
			N360S (Transverse)	0.827
Kobe, 1995	January 17th, 1995	JMA	EW (Longitudinal)	0.617
			NS (Transverse)	0.818

* PGA = Peak ground acceleration

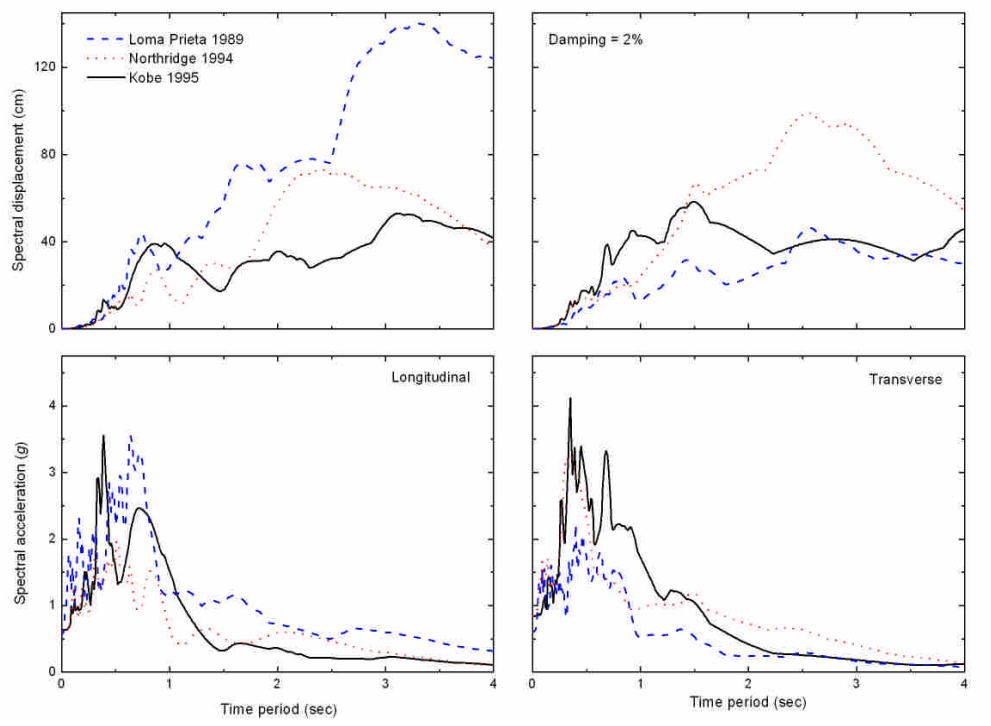

Figure 3. Displacement and acceleration spectra of three earthquake ground motions applied in longitudinal and transverse direction of the bridge.

Table 2. Peak response of bridge in isolated and non-isolated conditions with and without asymmetries.

Earthquake motion	Isolation system	Direction	Abutment base shear (W_d)			Deck displacement (cm)		Deck acceleration (g)		
			Non-isolated	Isolated		Abutment		Non-isolated	Isolated	
				Uncoupled	Coupled	Uncoupled	Coupled		Uncoupled	Coupled
Loma Prieta, 1989	LRB	Longitudinal	0.513	0.133	0.133	53.62	53.62	1.915	0.545	0.545
		Transverse	0.325	0.076	0.073	19.27	16.76	1.214	0.195	0.179
	N-Z	Longitudinal	0.513	0.127	0.127	52.70	52.65	1.915	0.362	0.362
		Transverse	0.325	0.059	0.057	19.47	16.30	1.214	0.151	0.140
	FPS	Longitudinal	0.513	0.136	0.135	53.39	53.37	1.915	0.362	0.363
		Transverse	0.325	0.062	0.060	21.06	18.24	1.214	0.168	0.159
Northridge, 1994	LRB	Longitudinal	0.357	0.101	0.101	34.06	34.06	1.325	0.342	0.342
		Transverse	0.483	0.143	0.138	49.55	46.47	1.975	0.501	0.486
	N-Z	Longitudinal	0.357	0.090	0.090	46.66	45.72	1.325	0.313	0.315
		Transverse	0.483	0.111	0.109	55.36	52.32	1.975	0.385	0.371
	FPS	Longitudinal	0.357	0.099	0.093	51.97	50.50	1.325	0.346	0.352
		Transverse	0.483	0.125	0.110	65.48	53.90	1.975	0.457	0.378
Kobe, 1995	LRB	Longitudinal	0.310	0.073	0.073	16.59	16.59	1.069	0.172	0.172
		Transverse	0.549	0.102	0.104	32.58	29.54	2.101	0.338	0.334
	N-Z	Longitudinal	0.310	0.066	0.066	17.14	17.08	1.069	0.130	0.130
		Transverse	0.549	0.077	0.074	28.23	26.14	2.101	0.207	0.192
	FPS	Longitudinal	0.310	0.071	0.071	16.78	16.78	1.069	0.133	0.134
		Transverse	0.549	0.072	0.069	25.73	24.50	2.101	0.211	0.187

Similar observations can be made from Figures 4, 5, and 6 showing variation of the peak values of shear force developed in the abutment, acceleration induced in the bridge deck, transverse displacement of CM and displacement of corner of the bridge deck against the eccentricity ratio, e_{xb}/d under 1989 Loma Prieta, 1994 Northridge and 1995 Kobe earthquakes while keeping $e_{xf}/d = 0$. The bridge properties and respective isolation properties of LRB, N-Z and FPS are maintained the same as previous. The frequency ratios are chosen such as $\Omega = 0.8, 1, 1.5, 2$ representing the torsionally flexible to torsionally stiff bridge. In addition, it is observed that the displacement of corner of the bridge deck increases with increasing isolation eccentricity arising due to the isolator stiffness. The displacement of corner of the bridge deck governs the isolation gap required to avoid mutual pounding of the bridge deck during earthquakes.

Moreover, Figures 7 and 8 show responses obtained for the isolation eccentricity developed due to dissimilarities in the isolator yield forces, with $\Omega = 0.8, 1, 1.5, 2$. The variation of the peak values of shear force developed in the abutment, acceleration induced in the bridge deck, transverse displacement of CM and displacement of corner of the bridge deck are plotted against the eccentricity ratio,

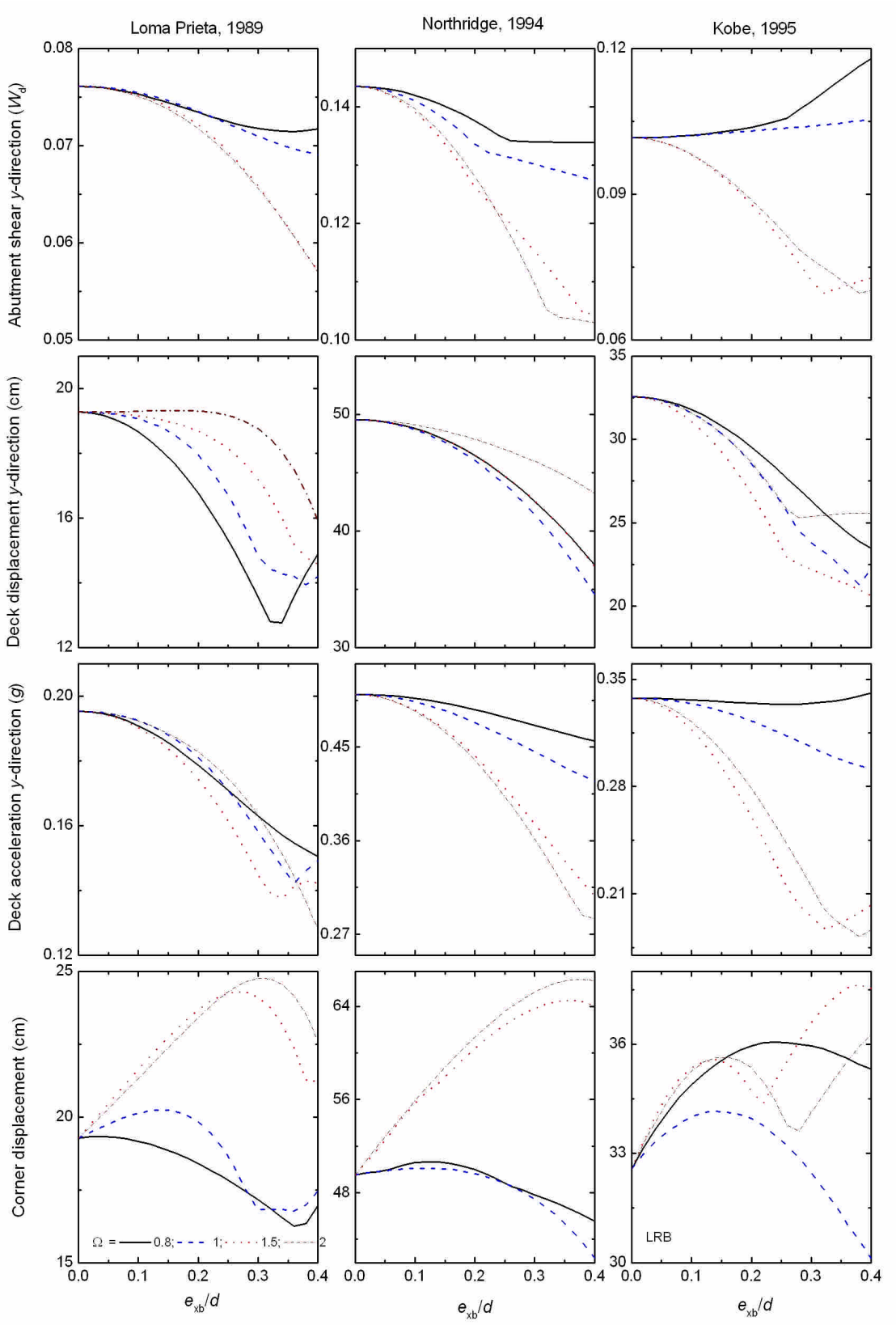

Figure 4. Seismic response of the base-isolated bridge against the eccentricity due to the isolation stiffness in LRB.

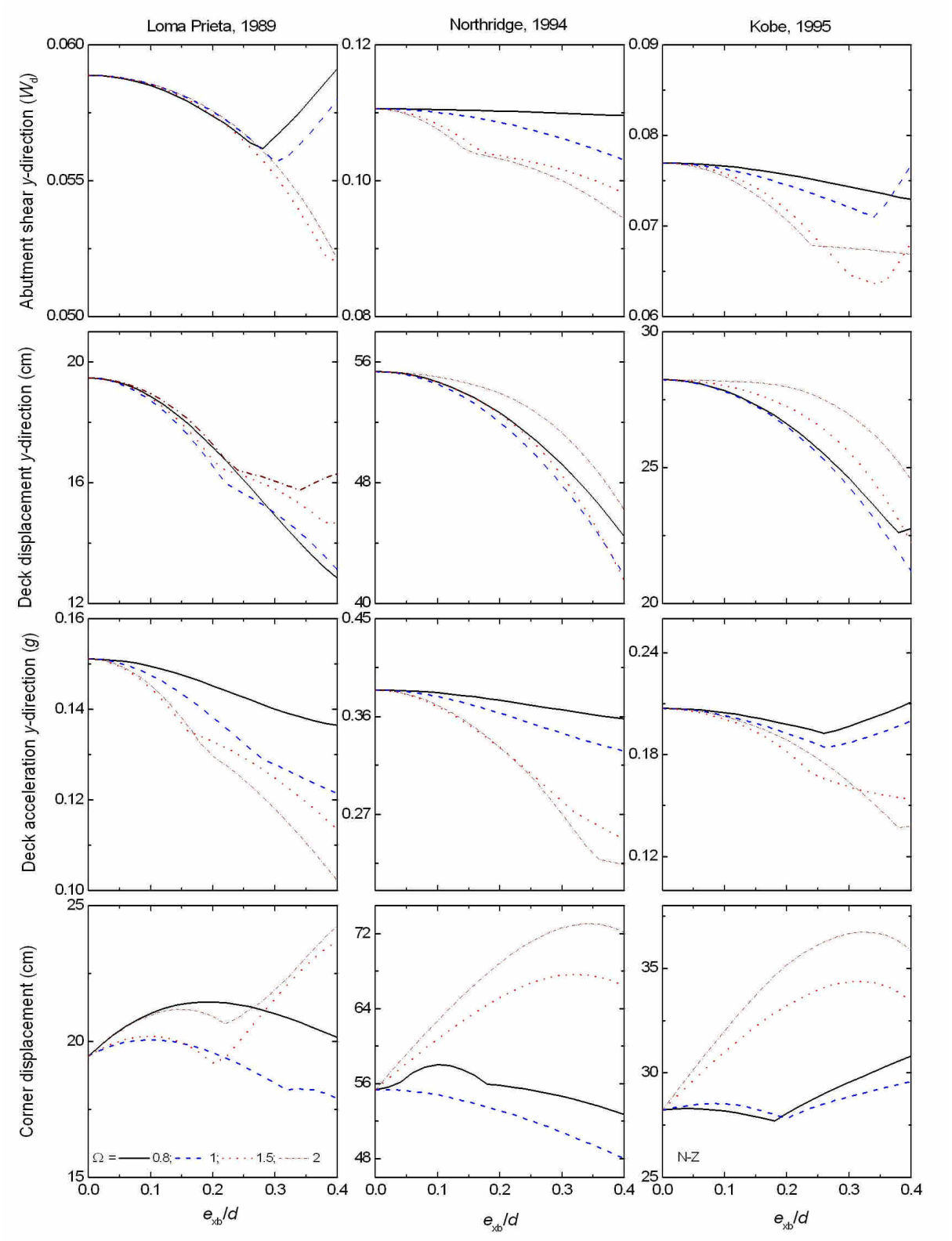

Figure 5. Seismic response of the base-isolated bridge against the eccentricity due to the isolation stiffness in N-Z system.

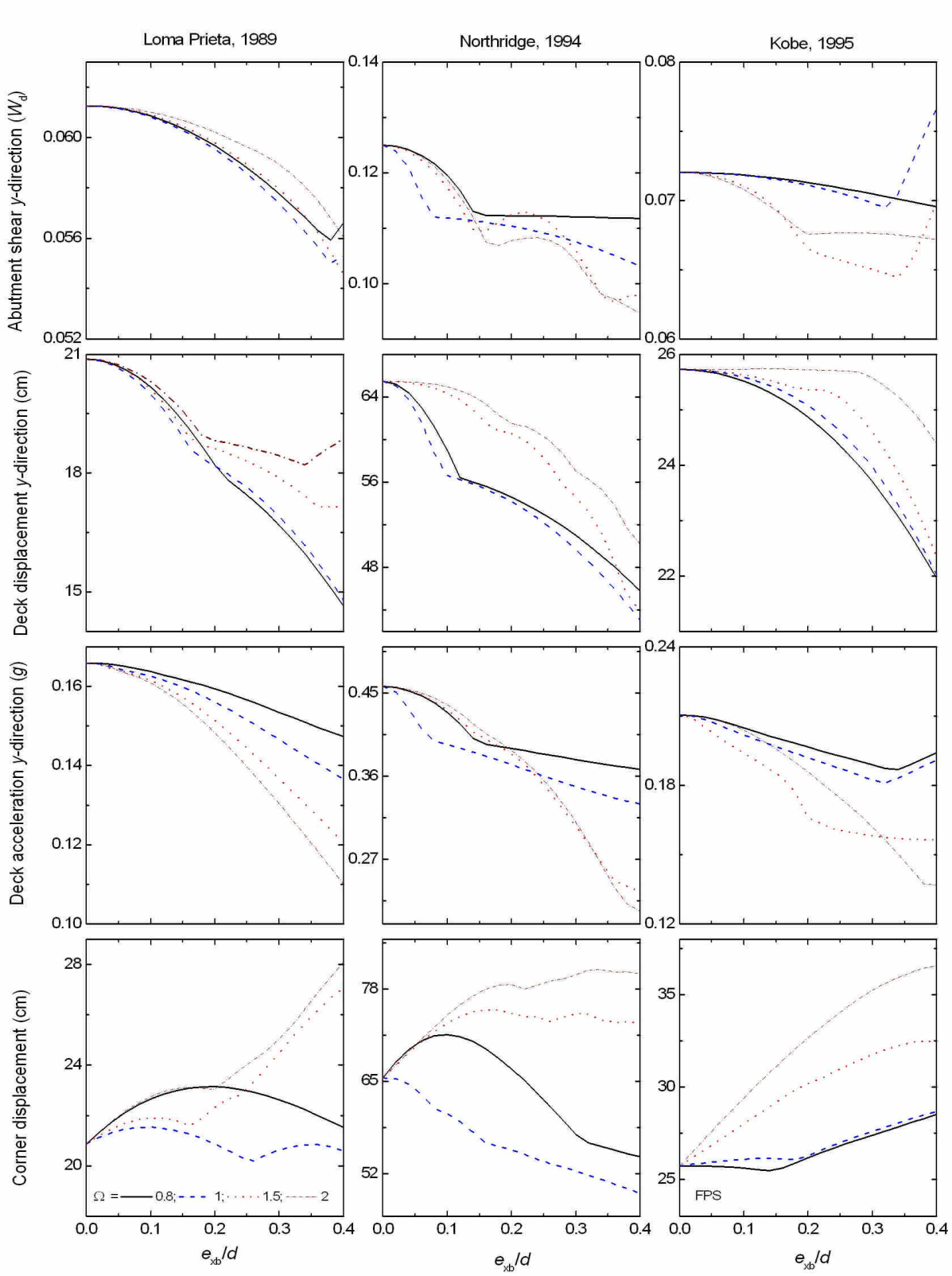

Figure 6. Seismic response of the base-isolated bridge against the eccentricity due to isolation stiffness in FPS.

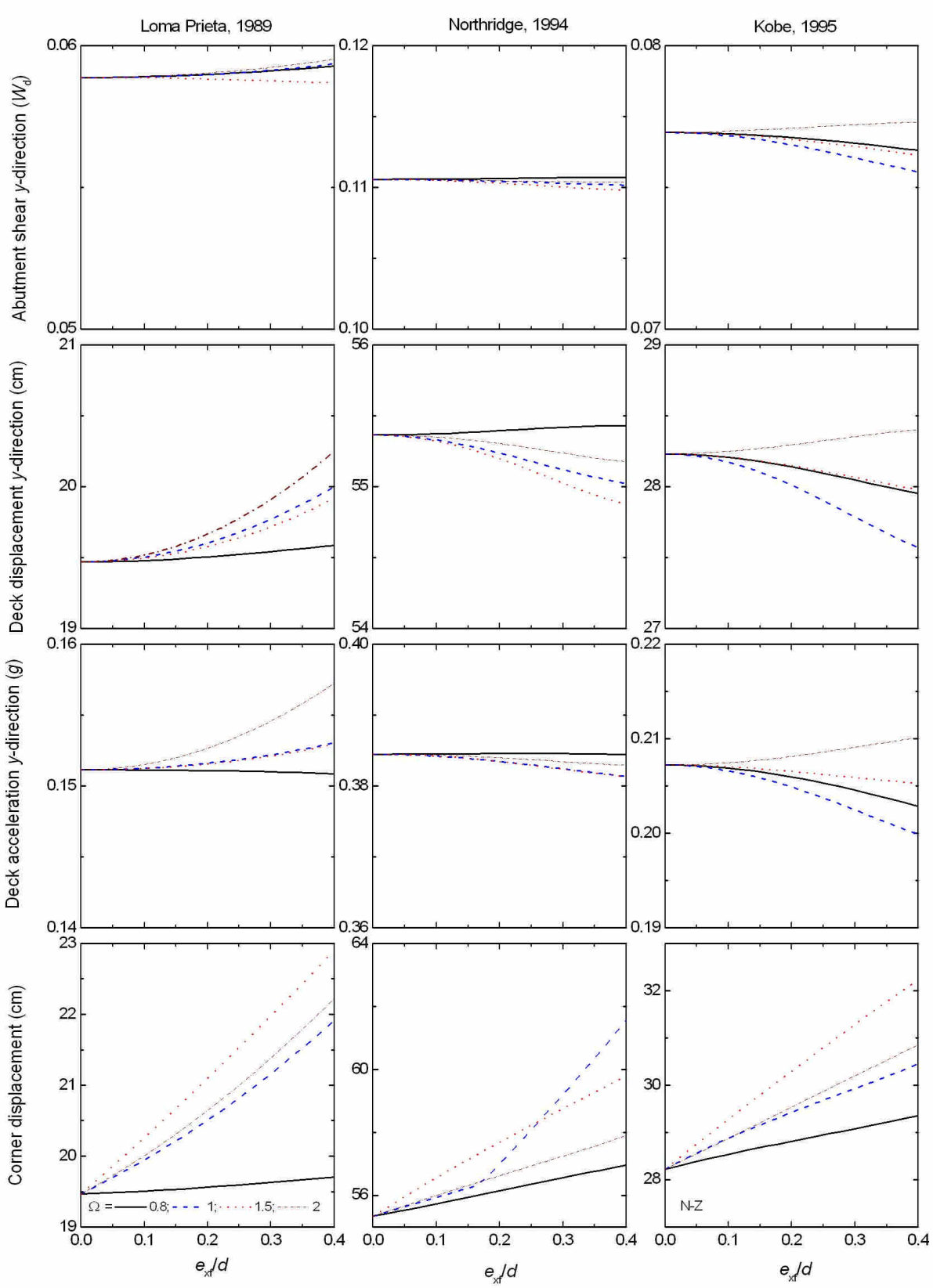

Figure 7. Seismic response of the base-isolated bridge against the eccentricity due to isolator yield forces in N-Z system.

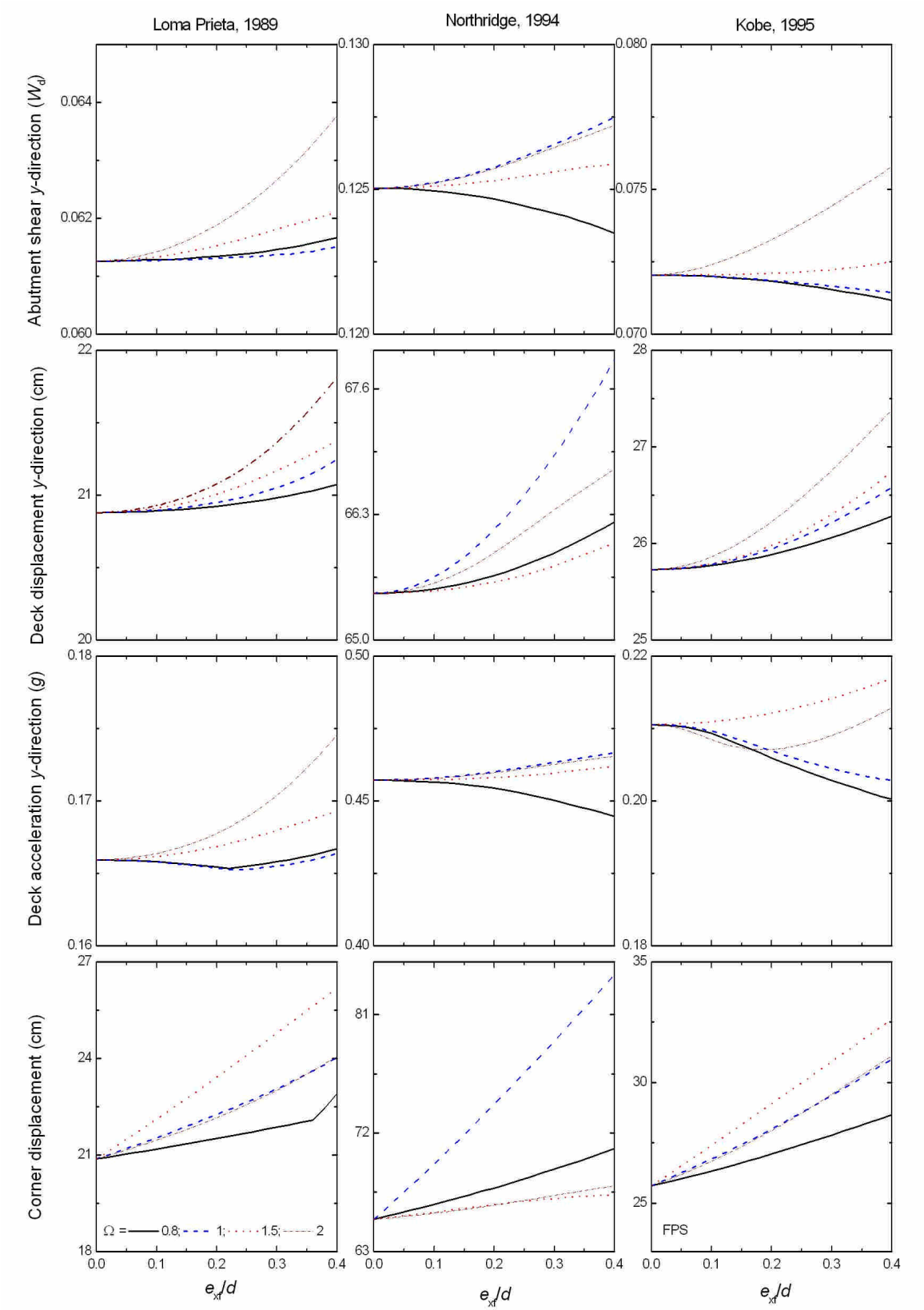

Figure 8. Seismic response of the base-isolated bridge against the eccentricity due to the isolator yield forces in FPS.

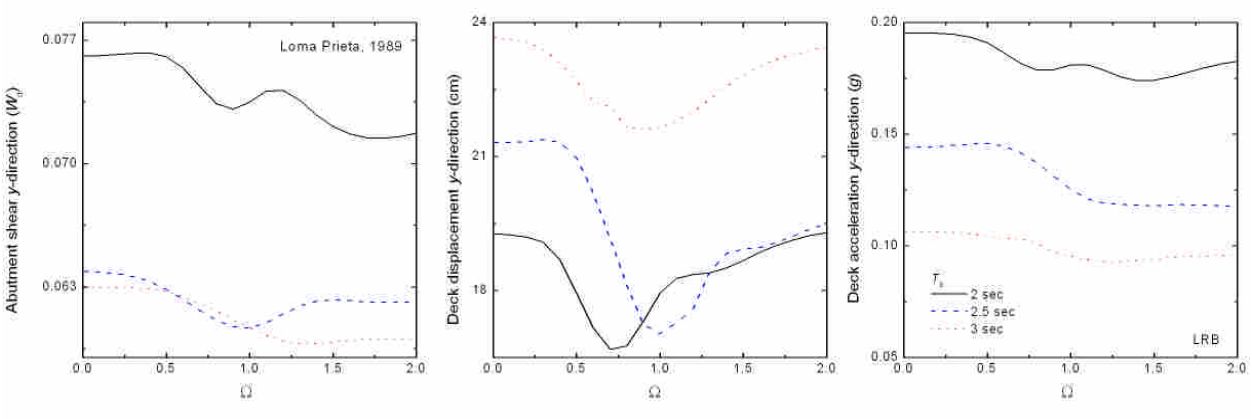

Figure 9. Seismic response of the base-isolated bridge against the frequency ratio for LRB.

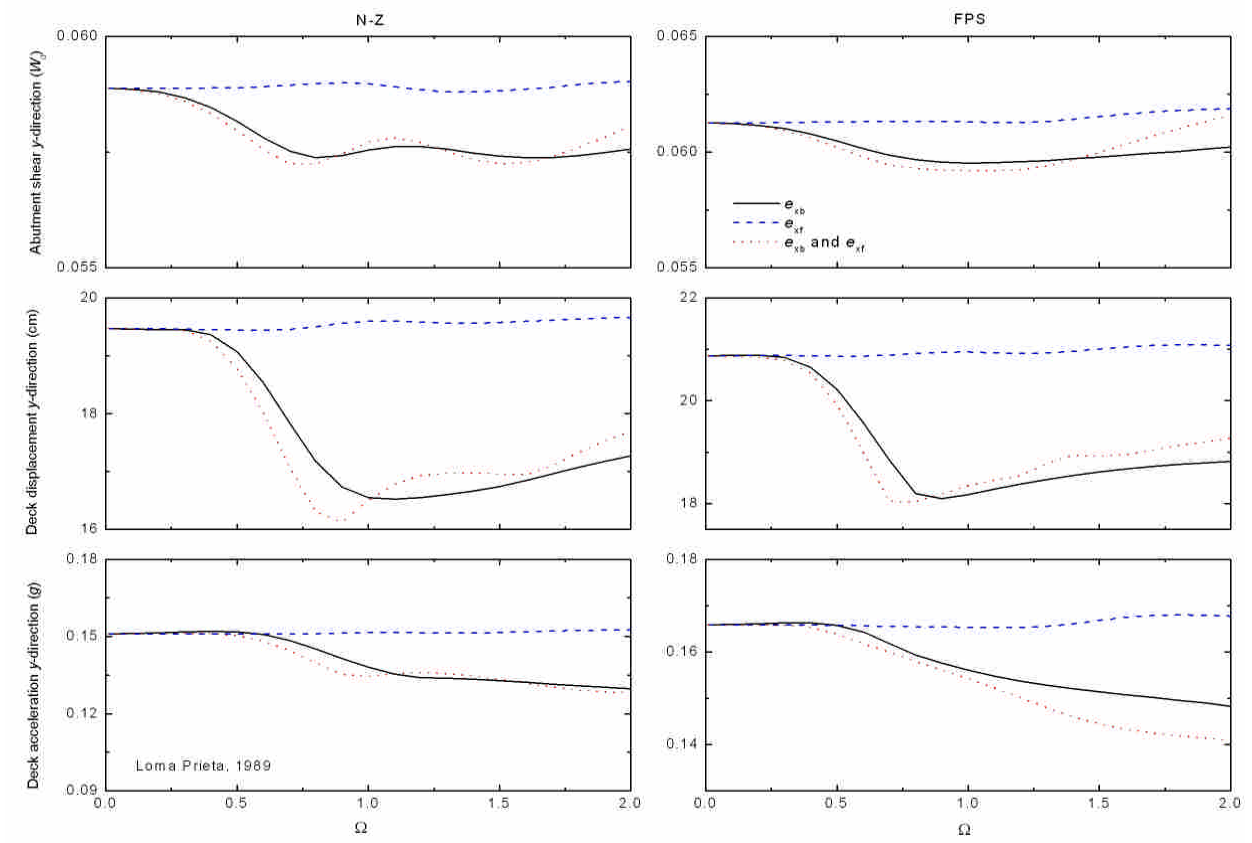

Figure 10. Seismic response of the base-isolated bridge against the frequency ratio for N-Z and FPS.

e_{xf}/d while keeping $e_{xb}/d = 0$ under 1989 Loma Prieta, 1994 Northridge and 1995 Kobe earthquakes. The respective isolation systems utilized here are N-Z and FPS with isolation parameters kept the same as previous. It is observed that the displacement of corner of the bridge deck increases almost linearly with the increasing isolation eccentricity; which would have been ignored in 2D analysis, thereby under-predicting requirement of isolation gap. Such under-prediction of isolation gap and its subsequent provision leads to seismic pounding and possible catastrophic

dislodgement failures during earthquakes. Figures 5 and 6 when compared with Figures 7 and 8, it is seen that the effects of the isolation eccentricity arising due to the isolator yield forces are inferior as compared to those arising due to the isolator stiffness.

Figure 9 shows the effect of ratio between the torsional frequency and the lateral frequency on the seismic response of the bridge with LRB under Loma Prieta, 1989 earthquake. For the bridge with LRB, different isolation time periods, T_b= 2, 2.5, 3 sec are chosen. The isolation eccentricity, $e_{xb}/d = 0.2$, is selected with isolation parameters kept the same as previous. It is seen that with increasing torsional to lateral frequency ratio, the seismic response goes on decreasing implying thereby that torsionally flexible bridge shows more coupling effects than those of the torsionally rigid bridge.

Figure 10 shows the effect of ratio between the torsional frequency and the lateral frequency on the seismic response of the bridge with N-Z and FPS under Loma Prieta, 1989 earthquake. The response for N-Z and FPS belongs to the presence of various eccentricities such as $e_{xb}/d, e_{xf}/d$ individually or in the presence of both simultaneously. The isolation eccentricities of $e_{xb}/d = 0.2$ and $e_{xf}/d = 0.2$ are considered as applicable, with isolation parameters keeping the same as previous. Here also, it is seen that with increasing torsional to lateral frequency ratio, the seismic response goes on decreasing showing effects of increased frequency ratio. Noticeably, these plots also brings forward that the torsional coupling arising because of the dissimilarity in the stiffness of the isolators is affected more to the changes in the frequency ratio than that due to the yield forces in the isolators.

5. Conclusions

The torsional coupling arising due to the mismatch of isolation stiffness and/ or yield forces of the seismic isolators in the simply supported base-isolated bridges is formulated and discussed here. Following conclusions are arrived at from the study of seismic response of torsionally coupled base-isolated bridge subjected to bi-directional earthquake ground motions.

1. The eccentricities arising due to the dissimilar isolator properties (isolation stiffness and/ or yield forces) in the base-isolated bridge affects its seismic response considerably.
2. The effectiveness of isolation reduces at higher eccentricities due to the asymmetries in the isolator properties, and the effectiveness of isolation will be over-predicted if these eccentricities are ignored. Inclusion of the isolation eccentricities in the analysis leads to correct estimation of the effectiveness of isolation and appropriate provision of the isolation gaps to avoid seismic pounding.
3. The eccentricity arose due to the variation in isolation stiffness affects the seismic response more severely than that due to the isolator yield forces.
4. The torsionally coupled seismic response diminishes with increasing torsional to lateral frequency ratio.

References

[1] Ghobarah, A. and Ali, H.M. 1988. Seismic Performance of Highway Bridges. *Engineering Structures*, 10(3), 157-166.

[2] Turkington, D.H., Carr, A.J., Cooke, N. and Moss, P.J. 1988. Seismic Design of Bridges on Lead-Rubber Bearings. *Journal of Structural Engineering*, ASCE, 115, 3000-3016.

[3] Hwang, J.S. and Sheng, L.H. 1994. Equivalent Elastic Seismic Analysis of Base-Isolated Bridges with Lead-Rubber Bearings. *Engineering Structures*, 16(3), 201-209.

[4] Kartoum, A., Constantinou, M.C., and Reinhorn, A.M. 1992. Sliding Isolation

System for Bridges: Analytical Study. *Earthquake Spectra*, 8(3), 345-372.

[5] Wang, Y.P., Chung, L.L., and Liao, W.H. 1998. Seismic Response Analysis of Bridges Isolated with Friction Pendulum Bearings. *Earthquake Engineering and Structural Dynamics*, 27(10), 1069-1093.

[6] Jangid, R.S. 2004. Seismic Response of Isolated Bridges. *Journal of Bridge Engineering*, ASCE, 9(2), 156-166.

[7] Kunde, M.C. and Jangid, R.S. 2003. Seismic Behavior of Isolated Bridges: A State-of-the-Art Review. *Electronic Journal of Structural Engineering*, 3, 140-170.

[8] Jangid, R.S. 1996. Seismic Response of an Asymmetric Base Isolated Structure. *Computers and Structures*, 60(2), 261-267.

[9] Jangid, R.S. 2000. Seismic Response of Structures with Sliding Systems. *Journal of Seismology and Earthquake Engineering*, 2(2), 45-54.

[10] Jangid, R.S. and Kelly, J.M. 2000. Torsional Displacements in Base-Isolated Buildings. *Earthquake Spectra*, 16(2), 443-454.

[11] Ryan, K.L. and Chopra, A.K. 2004. Estimation of Seismic Demands on Isolators in Asymmetric Buildings using Non-Linear Analysis. *Earthquake Engineering and Structural Dynamics*, 33(3), 395-418.

[12] Kunde, M.C. and Jangid, R.S. 2006. Effects of Pier and Deck Flexibility on the Seismic Response of Isolated Bridges, *Journal of Bridge Engineering*, ASCE, 11(1), 109-121.

[13] Matsagar, V.A. 2005. Earthquake Behavior and Impact Response Control of Base-Isolated Buildings. *PhD Thesis*, Indian Institute of Bombay, India.

[14] Simo, J.C. and Kelly, J.M. 1984. The Analysis of Multilayer Elastomeric Bearings. *Journal of Applied Mechanics*, ASME, 51(2), 244-250.

[15] Skinner, R.I., Kelly, J.M. and Heine, A.J. 1975. Hysteretic Dampers for Earthquake-Resistant Structures. *Earthquake Engineering and Structural Dynamics*, 3(3), 287-296.

[16] Robinson, W.H. 1982. Lead-Rubber Hysteretic Bearings Suitable for Protecting Structures During Earthquakes. *Earthquake Engineering and Structural Dynamics*, 10(4), 593-604.

[17] Park, Y.J., Wen, Y.K., and Ang, A.H.-S. 1986. Random Vibration of Hysteretic Systems under Bi-Directional Ground Motions. *Earthquake Engineering and Structural Dynamics*, 14(4), 543-557.

[18] Nagarajaiah, S., Reinhorn, A.M., and Constantinou, M.C. 1991. Nonlinear Dynamic Analysis of 3-D Base-Isolated Structures. *Journal of Structural Engineering*, ASCE, 117 (7), 2035-2054.

[19] Jangid, R.S. and Datta, T.K. 1994. Nonlinear Response of Torsionally Coupled Base Isolated Structure. *Journal of Structural Engineering*, ASCE, 120(1), 1-22.

[20] Zayas, V.A, Low, S.S., and Mahin, S.A. 1990. A Simple Pendulum Technique for Achieving Seismic Isolation. *Earthquake Spectra*, 6(2), 317-333.